

# From inert gas to fertilizer, fuel and fine chemicals: N<sub>2</sub> reduction and fixation

Artur Braun <sup>1</sup>, Debajeet Kumar Bora <sup>2</sup>, Lars Lauterbach<sup>3</sup>, Elisabeth Lettau <sup>3</sup>, Hongxin Wang <sup>4</sup>,

Stephen P. Cramer <sup>4</sup>, Feipeng Yang <sup>5</sup>, Jinghua Guo <sup>5</sup>

<sup>1</sup>Empa, Swiss Federal Laboratories for Materials Science and Technology

Laboratory for High Performance Ceramics

Überlandstrasse 129, CH-8600 Dübendorf, Switzerland

[artur.braun@alumni.ethz.ch](mailto:artur.braun@alumni.ethz.ch)

<sup>2</sup> Artificial Photosynthesis Research Group, Centre for Nano and Materials Sciences

JAIN (Deemed to be University), Bangalore, India

[debajeet1@hotmail.com](mailto:debajeet1@hotmail.com)

<sup>3</sup> Technische Universität Berlin/ Institute for Chemistry, Max-Volmer-Laboratorium, Sekr. PC 14

Strasse des 17. Juni 135, 10623 Berlin, Germany

[lauterbl@win.tu-berlin.de](mailto:lauterbl@win.tu-berlin.de) , [elisabeth.lettau@tu-berlin.de](mailto:elisabeth.lettau@tu-berlin.de)

<sup>4</sup> SETI Institute, 189 Bernardo Ave, Suite 200, Mountain View, CA 94043, United States

[hongxin.ucd@gmail.com](mailto:hongxin.ucd@gmail.com) , [spcramer@mac.com](mailto:spcramer@mac.com)

<sup>5</sup> Advanced Lightsource, Lawrence Berkeley National Laboratory, One Cyclotron Road, Berkeley

CA 94720, United States

[jguo@lbl.gov](mailto:jguo@lbl.gov) , [feipeng\\_yang@lbl.gov](mailto:feipeng_yang@lbl.gov)

This document is the accepted manuscript version of the following article:

Braun, A., Bora, D. K., Lauterbach, L., Lettau, E., Wang, H., Cramer, S. P., ... Guo, J. (2021). From inert gas to fertilizer, fuel and fine chemicals: N<sub>2</sub> reduction and fixation. *Catalysis Today*. <https://doi.org/10.1016/j.cattod.2021.04.020>

- 1 -

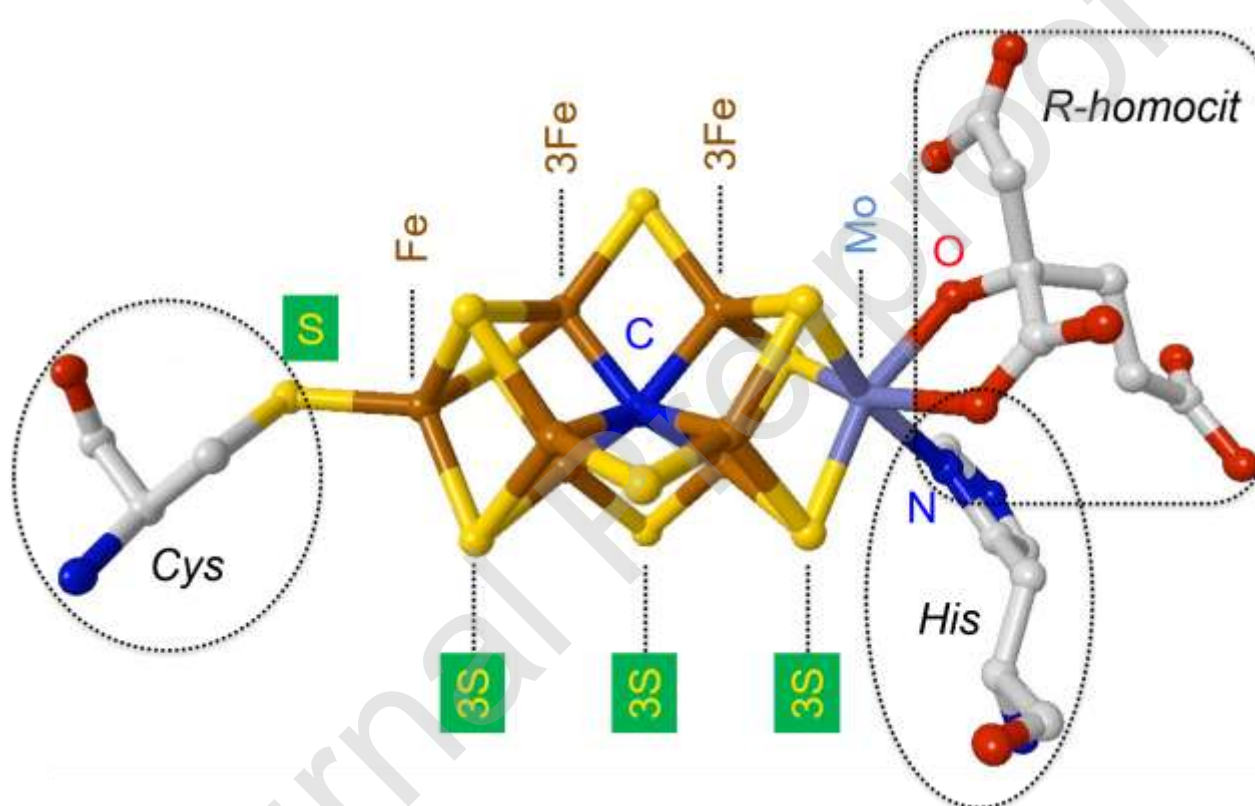
This manuscript version is made available under the CC-BY-NC-ND 4.0 license <http://creativecommons.org/licenses/by-nc-nd/4.0/>

## Corresponding author

Dr. Artur Braun

Tel.: +41 58 765 4850; Fax: +41 58 765 4150; e-mail: [artur.braun@alumni.ethz.ch](mailto:artur.braun@alumni.ethz.ch)

## Graphical abstract



## Highlights

- Electrochemical ammonia synthesis
- Vibration structure of nitrogenase protein
- Outlook on ammonia economy

## Abstract

The 100<sup>th</sup> anniversary of a leading nitrogen fixation technology developer like CASALE SA is a reason to reflect over the 20<sup>th</sup> century successful solution of the problem of world food supply, and to look out for solutions for sustainable developments with respect to ammonia production. We review the role of nitrogen as essential chemical constituent in photosynthesis and biology, and component of ammonia as it is used as fertilizer for primary production by photosynthesis for farming and food supply and its future role as energy carrier. While novel synthesis methods and very advanced synchrotron based x-ray analytical techniques are being developed, we feel it is important to refer to the historical and economical context of nitrogen. The breaking of the  $\text{N}\equiv\text{N}$  triple bond remains a fundamental chemical and energetic problem in this context. We review the electrochemical ammonia synthesis as an energetically and environmentally benign method. Two relatively novel X-ray spectroscopy methods, which are relevant for the molecular understanding of the catalysts and biocatalysts, i.e. soft X-ray absorption spectroscopy and nuclear resonant vibration spectroscopy are presented. We illustrate the perceived reality in fertilizer usage on the field, and fertilizer production in the factory complex with photos and thus provide a contrast to the academic view of the molecular process of ammonia function and production.

## Keywords

Nitrogen, Ammonia, Electrochemistry, Synchrotron, Nitrogenase, Catalysis

## Introduction

The 100<sup>th</sup> anniversary of a leading nitrogen fixation technology developer like CASALE SA is a reason to reflect over the 20<sup>th</sup> century successful solution of the problem of world food supply. It is also the opportunity to project on an issue of the beginning 21<sup>st</sup> century, this is, the sustainability in ammonia production. This paper recalls and reviews the historical aspects of urea and ammonia synthesis; in particular, the motivation of researchers to artificially fix nitrogen from air to produce synthetic fertilizers. Underlying is a key process in chemical engineering, the accomplishment of which was awarded with a Nobel Prize, followed by unprecedented food production and growth of world population. Since the process is energy intensive and primarily based on fossil fuel usage, the need for sustainable processes has been voiced louder in the previous decades. In addition, the extension of nitrogen fixation technologies, for example for the production of ammonia fuel or for fine chemicals, has been proposed. We complement the historical overlook in this review with the novel developments in electrochemical ammonia synthesis and in x-ray analytical methods which help elucidate the molecular processes in nitrogen chemistry. Seemingly trivial information in this review has been added for didactic purposes.

Nitrogen is abundant in the atmosphere to almost 80% as gaseous N<sub>2</sub>. In many fields of technology and industry, N<sub>2</sub> is considered and utilized as an inert gas. Nitrogen is one of the most important chemical elements in living systems, as we will outline below. It is an essential component of all amino acids, the building blocks of the proteins, which catalyze virtually all metabolic processes and thereby enable life. Life would not work the way we know it if it was without the nitrogen atom. Furthermore, nitrogen is contained in many other essential biological molecules like porphyrin rings, cytochromes, chromophores, and DNA. Nitrogen has five valence electrons (2s<sup>2</sup> 2p<sup>3</sup>) and forms only three bonds, for example with the three protons in ammonia NH<sub>3</sub>. The main source for

nitrogen is molecular nitrogen gas  $N_2$ , with its formal oxidation state 0. The oxidation state of nitrogen can vary between +5 and -3. In ammonia, N has the valence -3, whereas in nitrates the valence is +5. In the ammonium nitrate fertilizer  $NH_4NO_3$ , the valence of N is -3 and +5, respectively. Amines, the derivatives of ammonia, may have valences from -3 to -1 for N depending on particular side chains. The metabolism in vertebrates converts the toxic ammonia into the physiologically more benign urea, where N has also the valence -3. This oxidation state for N is prevalent also for the amino acids, which are the building blocks for proteins. Although highly abundant in the atmosphere, the availability of nitrogen for organisms is limited. The reason for this is that the molecular nitrogen must be fixed in the form of ammonia to become metabolic useable; a task that can be performed only by diazotrophic bacteria. Because of most organisms are not able to fix nitrogen to ammonia, they must assimilate nitrogen in the form of nitrate leading to ammonium formation or directly as ammonium. Ammonia is then converted to glutamate or/and glutamine. All other amino acids are synthesized by transamination reactions from these building blocks. Amino acids serve as basis for the synthesis of a number of different biological nitrogen containing bioactive compounds such as pyrrolidines, piperazines and piperidines, which are important precursors of pharmaceuticals and agrochemicals. Here, especially the piperazine scaffold is a privileged structural motif in drug discovery and continues to have an increasing appearance in lifesaving drug molecules, e.g. in *Imatinib* for leukemia treatment or *Levocetirizine*, which is an antihistamine [1].

Figure 1 shows on the left the cytochrome c, which transfers electrons within the respiratory chain. Nitrogen is an essential chemical element in the porphyrin molecules, aromatic rings with particular color centers, such as heme, which is the cofactor of haemoglobin and which gives the red blood cells their color. Heme has the life critical function of binding oxygen to the bloodstream of vertebrates. On the right in Figure 1, the iron porphyrin ring contains Fe as the central atom, which we know as heme.

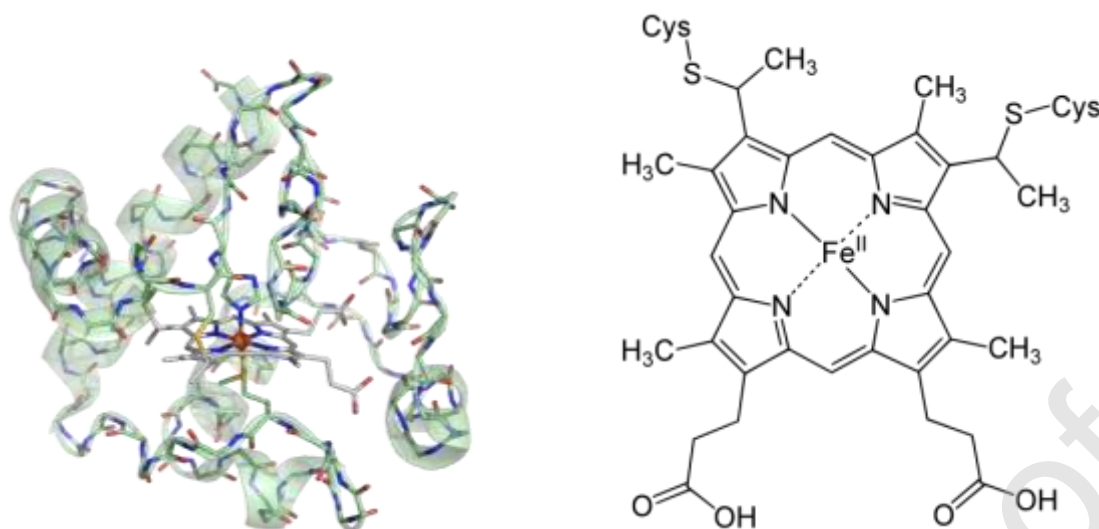


Figure 1: (left) Structure of cytochrome *c* (green) with a heme *c* molecule with the peptide backbone and heme *c* cofactor (grey) coordinating a central Fe atom (orange sphere). (right) The heme *c* molecule with Fe as central atom. Nitrogen atoms are depicted in blue, oxygen atoms in red and sulphur atoms in yellow and iron in orange as a sphere. Alpha-helices are transparent. For simplification, only the main chain is shown except the two cysteines bound to heme *c* and methionine and histidine coordinating side chains of the cofactor.

Urea ( $\text{CO}(\text{NH}_2)_2$ ) is the decay product of proteins in animal and human metabolism and was (by intent) first synthesized in the laboratory by Friedrich Wöhler in 1828 [2] (see also [3]), not very long before Justus von Liebig pointed out the importance that nitrogen was an essential fertilizer in agriculture [4]. Still today, farmers distribute the waste from their animals as solid and liquid manure over the farmland. Such "green farming" has been practised for thousands of years [5], and farmers were constantly in need for natural fertilizer. Shortage could contribute to undernourishment and eventually to famine (during the big leap famine in People's Republic of China, farmers were desperately searching for every tiny bit of animal or human manure [6]), which was one rational to – in addition - look out for mineral and synthetic fertilizers. Without synthetic fertilizer, there will not

be enough food for today's population [7]. Already over 100 years ago, Sir William Crookes predicted famine in near future unless care was taken of agriculture management. Crookes considered manure a treasure and cited Justus von Liebig with "Nothing will more certainly consummate the ruin of England than a scarcity of fertilisers - it means a scarcity of food." [8]. Today, around 1% of mankind's global energy consumption is spent for ammonia production in large centralized plants with 2500 tons production per day, and a total global  $\text{NH}_3$  production of 146 million tons per year [9], Casale SA being one of the technology companies which build the factories. Synthetic urea, too, is a fertilizer today produced in huge quantities. Still, manure is being used as fertilizer. Figure 2 shows an example from the year 2020 in the highly industrialized Switzerland.



Figure 2: Local farmer spreading liquid manure (natural nitrogen fertilizer) over a meadow in the Canton of Zurich, Switzerland. Photo Artur Braun, 3 April 2020.

### **Haber-Bosch ammonia synthesis and similar processes**

With proceeding industrialization, it became clear that nitrogen was a critical resource, and ammonia  $\text{NH}_3$  a key chemical product for further technological development [10]. As one of the most produced chemicals, ammonia ( $\text{NH}_3$ ) synthesis through the Haber-Bosch process is capital and



energy intensive and constitutes 1-2% of the entire energy consumption in the world [11-13]. In 1910, Fritz Haber succeeded with the synthesis of ammonia in a catalysed reaction of  $\text{H}_2$  and  $\text{N}_2$  under high temperature and pressure [14-16], which became commercialized as the Haber-Bosch process. Back then, it was not trivial to build vessels that could maintain a pressure of  $250 \pm 100$  bar at temperatures of  $400^\circ\text{C}$  to  $500^\circ\text{C}$  to allow for the chemical conversion of nitrogen and hydrogen to ammonia. A replica of the original experimental setup which Haber used for ammonia synthesis is shown in the photo in Figure 3 and originally sketched in the paper which Haber co-authored with his British colleague Robert Le Rossignol [15]. The paper was originally a report produced for BASF chemical company in 1909, 3 ½ years prior to publication.



Figure 3: Replica of the apparatus for the Haber Bosch ammonia process, at the Fritz Haber Institut in Berlin-Dahlem. The sketch of the apparatus is shown in the original paper by Haber and Le Rossignol [15]. Photo Artur Braun, 9 November 2014.



Similar ammonia synthesis processes followed, including the Casale process [17, 18]. Luigi Casale worked also on the preparation of iron catalysts for the ammonia synthesis. Ammonia synthesis allowed for the production of synthetic mineral nitrogen fertilizer, which coined the phrase "bread from air" [19]. Since, world population has increased virtually exponential to over 7 billion humans. Thus, the problem of feeding the people on the globe is solved with respect to one critical bottleneck: by using synthetic fertilizer in agriculture technology. For large countries with a large population and wide farmlands, independent fertilizer production capacity is crucial and an opportunity to become partially independent from food imports. Notwithstanding that there are further issues to be considered, such as understanding the dynamics of soil, crops and fertilizers, and its implications for success of farming [20]. Figure 4 shows an ammonia/urea production plant in the city of Allahabad, owned by the Indian Farmers Fertilizer Cooperative IFFCO. Such factories may require an area of up to 1 square kilometre or even more, and do resemble the complexity of the plant cells in photosynthesis, both of which require tubes and paths for transport and vessels for reactions.



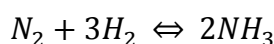
Figure 4: The Phulpur ammonia factory in Allahabad, India. Photo from Casale SA. The size of the full industrial complex is around 800 m by 800 m.

Because of its wide applications, such as fertilizer source of nitrogen [21], a potential transportation fuel with no CO<sub>2</sub> emission and efficient clean energy carrier (due to its high energy density of 17.8%) [22, 23], several of sustainable routes have been developed, including electrochemical methods, which could directly convert renewable electricity into chemicals or chemical energy carriers.

### Nitrogen fixation in nature

It is striking that technical ammonia production requires high temperature and pressure, whereas nature performs the breaking of the N≡N triple bond under supposedly ambient conditions by the nitrogenase metalloproteins. The biomolecular environment in which nitrogen reduction and fixation takes place is an aggressive electrochemical one and thus less than ambient. It is therefore of great interest to explore the molecular mechanism which perform this task. X-ray spectroscopy methods are one class of analytical tools, which help elucidate such mechanisms, as we will learn later in this review. Common for the technical and natural ammonia synthesis is the presence of iron Fe as a catalyst. In the ammonia technology, the catalysts contain typically Fe, Mo, and their alloys and sometimes V.

Nature performs nitrogen fixation of ambient N<sub>2</sub> by nitrogen fixing bacteria. The chemical reaction is the combination of protons H<sup>+</sup> with N<sub>2</sub> towards ammonia and reads simply:

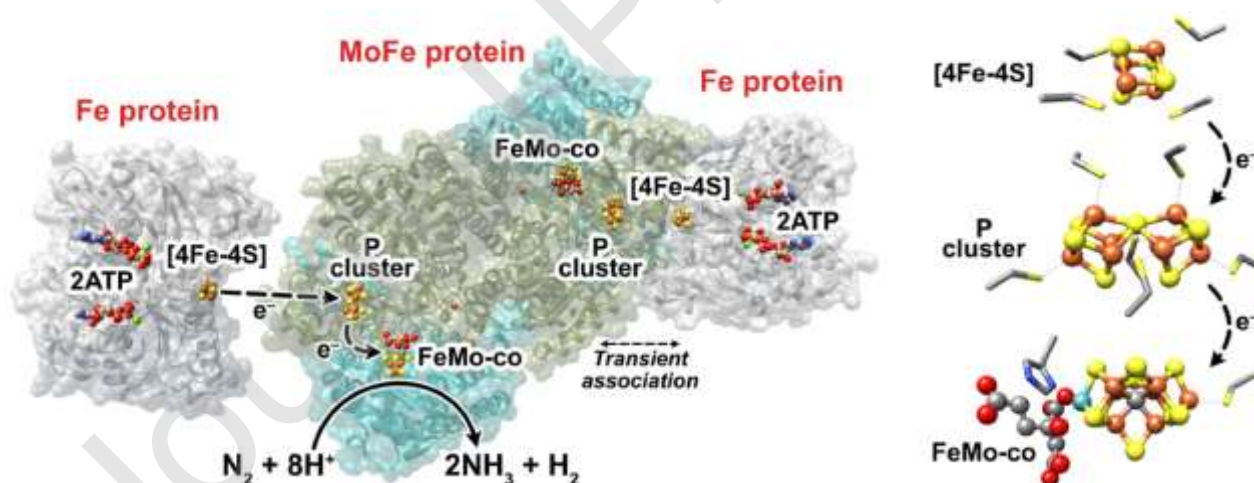


Such undifferentiated and oversimplified equation gives no account of the underlying problems that must be overcome to actually perform the reaction.

The production of ammonia requires the breaking of the nitrogen triple bond N≡N, which has an enormous bond energy of 941 kJ/mol. The necessary energy for industrial ammonia production

comes from fossil fuels, particularly natural gas, and from hydropower, the electricity of which is used to produce hydrogen by water electrolysis [24]. Hence, ammonia and urea production require enormous amounts of water and produce a large amount of CO<sub>2</sub>. This is why there is an interest in sustainable production of ammonia with renewables [9].

Nitrogen fixing bacteria like cyanobacteria (also known as blue green algae), for example *Anabaena* or bacteria like *Azotobacter*, contain the enzyme nitrogenase, which has the function of catalysing the nitrogen fixation by chemically reducing N<sub>2</sub> to NH<sub>3</sub>. The nitrogenase, as shown in the top panel in Figure 5, is a large macro-molecular complex, which contains several proteins, which reduce the N<sub>2</sub> to NH<sub>3</sub> by the transfer of six electrons (6 e<sup>-</sup> transfer). The center of the nitrogenase is an Fe-Mo protein (bottom in Figure 5) which performs the reduction, but it requires in its periphery two iron proteins which consume ATP to gain the energy to drive the required six electrons to the Fe-Mo complex.



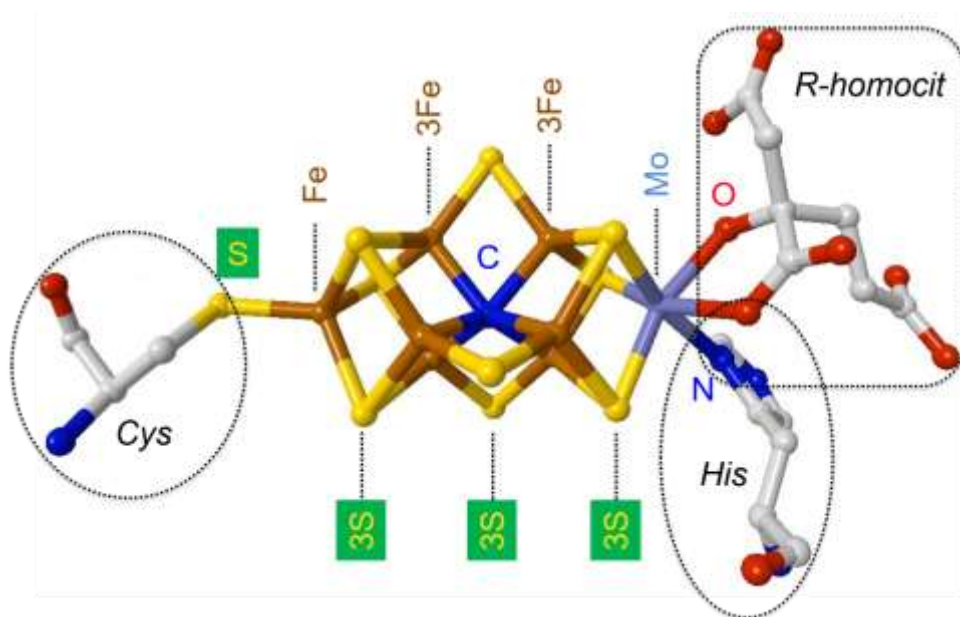


Figure 5: (top) Schematic of the nitrogenase protein complex (<https://www.mdpi.com/2624-8549/2/2/21#>). (bottom) Structure of the iron sulphur molybdenum co-factor.

Nitrogenase is the only known biological catalyst able to reduce  $N_2$  to  $NH_3$ . In the next section, we review the electrochemical synthesis of ammonia. Certainly, electrochemical methods are also used for electroanalytical studies of the nitrogenase function. For example, Hickey et al. have studied the reduction potentials of nitrogenase proteins immobilized on electrodes, and thus attempted to map the thermodynamic landscape of the active site of the Mo nitrogenase [25]. It has turned out over time that the large protein complexes, which make up life, contain a vibration structure and a shape, a form, which is followed by a mechanical function reminiscent of a machine literally bringing ions together for chemical reaction, which is necessary for driving the biochemical reactions [26]. This was discovered with a novel x-ray spectroscopy method. We therefore feature in this review particularly electrochemical ammonia synthesis, and novel synchrotron radiation based x-ray spectroscopy analytical techniques.

### Electrochemical synthesis of ammonia

The electrochemical synthesis of ammonia by nitrogen reduction reaction (NRR) is considered the best choice (by electrochemists!) due to its flexibility in tuning the input energy requirement as well as output products. Also, CO<sub>2</sub> emission does not take place which makes it an additional advantage, unless the necessary electric energy comes from combustion of fossil fuels and biomass. Interestingly, the same type of Fe catalysts in the Haber Bosch processes is used as homogenous and heterogeneous electrocatalysts for the green production of NH<sub>3</sub>. A simple electrochemical cell for the NRR reaction in ammonia synthesis is schematized in Figure 6.

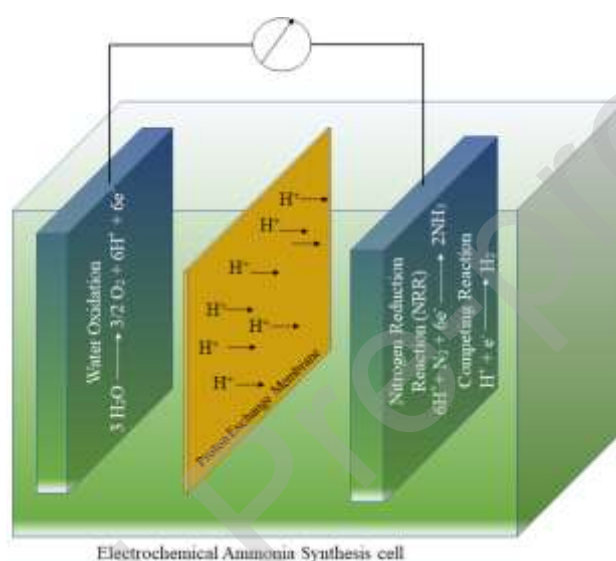


Figure 6: An electrochemical cell depicting the formation of ammonia from liquid electrolyte.

For the NRR reaction, a different range of materials is used for the design and development of electrocatalyst along with solid electrolytes. A concise and critical analysis of each of these electrocatalysts and solid electrolytes is discussed below in a chronological order until the recent state of the art. The main pros and cons of each of the electrocatalysts lies in the input voltage or overpotential, and faradaic efficiency associated with the NRR reaction. Another critical aspect to consider here is the correlation of the structure-selectivity factor for making ammonia specifically. The main cons of the NRR reaction with most of materials is the generation of side products of hydrogen



along with ammonia. Therefore, to control the same is the motivation of the most of the studies discussed below.

When we look back into history, Allen J. Bard et al. first developed the concept of heterogeneous nitrogen photoreduction into ammonia over stoichiometric  $\text{WO}_3$  photoanode by using moisturized  $\text{N}_2$ . The typical ammonia yield was  $0.1 \mu\text{g/h}$  [27]. Later, R.L. Cook et al. [28] reported the ambient temperature formation of electrochemical nitrogen reduction into ammonia over a Ru based catalysts with Pt as counter electrode separated by the Nafion membrane. They found a Faradaic (Coulombic) efficiency of 0.0015% for nitrogen-to-ammonia conversion with a current density of  $3.12 \text{ mA/cm}^2$ . In terms of final product concentration, they were able to generate  $1.75 \text{ nmoles/cm}^2/\text{h}$  on a  $10 \text{ cm}^2$  working electrode area. Various research work related to the green synthesis of ammonia was carried out in the last two decades. The work done by Kordali et al. [29] involved the production of ammonia by using Nafion membrane in the presence of Ru catalyst in an alkaline solution with an operation temperature of  $100^\circ\text{C}$ . The nitrogen reduction rate increased with the operating temperature.

Work by T. Murakami et al. shows formation of ammonia from water vapor and nitrogen in the molten ion-based electrolysis cell with electrolyte  $\text{LiCl-KCl-CsCl-Li}_3\text{N}$  (0.5 [30] mol%  $\text{Li}_3\text{N}$  added) [31]. Nitride ions are fed into the melt at the cathode, which reacts with water vapor and hence generates  $\text{NH}_3$ . The process efficiency was 23% in terms of current needed to generate ammonia. Computations [30] were carried out to identify the most suitable electrocatalyst for NRR. It was found that Mo nanoparticles are capable of forming ammonia, but with very high activation energy for nitrogen dissociation [32]. Due to the well-known effect of iron metal in Haber Bosch process, the ammonia synthesizes electrochemically by the electrolysis of air and steam in a hematite molten nano suspension [33]. The Coulombic efficiency obtained for this process was 35% at a temperature of  $200^\circ\text{C}$  and applied bias of 1.2 V. The cogeneration of hydrogen is evident here, and six electron conversion of nitrogen into ammonia is found.



Numerous reviews were written on the electrochemical synthesis of ammonia and the employed electrolytes and electrocatalysts. We want to show a glimpse of these before going to exciting electrocatalyst systems found recently for NRR reaction. The electrochemical synthesis of ammonia can be done with a wide range of electrolytes, spanning the range of liquid at ambient temperature to all solid electrolytes, see the review by Giddey et al. [34]. The number one is the liquid electrolyte near room temperature, followed by molten salt electrolyte operating at 300 °C - 500°C. Composite electrolyte, a blend of a traditional solid electrolyte with low melting point electrolyte, and finally all solid electrolyte which are able to carry out NRR at the higher range of temperature in a fuel cell setting (800°C). The hydrogen required for this purpose is fed to the anode separated by a ceramic membrane, which facilitates separation of hydrogen from ammonia by-product. The conventional Haber Bosch process is collecting this hydrogen from non-renewable energy sources, with a correspondingly large carbon footprint. M. Soukides et al. [35] made an extensive review on the use of perovskite structure metal oxide electrocatalysts, and even proton conductors such as  $\text{BaZr}_{0.8}\text{Y}_{0.2}\text{O}_{3-\delta}$  for ammonia generation. The drawback of these catalysts to carry out the NRR is the need for high temperature and their rare availability, and their toxic and expensive nature. Regarding this, we here subdivided many electrocatalysts system depending on the need of operating temperature into several categories. These are from high: greater than 500°C, medium: in between 100°C - 500°C and low temperature (100°C), while typical Haber Bosch process needs around 400-500 °C along with the pressure of 130-170 bar. Solid electrocatalyst such as  $\text{Fe}_2\text{O}_3$  deposited on activated carbon [36] is also used for ammonia generation in a high-temperature molten hydroxide electrolyte following the same. Activated carbon, the host material [30], opens the pathway necessary for increasing efficiency of the process. It is found that the  $\text{Fe}_2\text{O}_3$  /activated carbon inhibits the competing hydrogen evolution reaction along with the NRR. The operating temperature of the reaction process is 250°C, and the highest ammonia formation occurs at 1.55 V, with a current density of 49 mA/cm<sup>2</sup>. The fundamental understanding of the metal center of these electrocatalysts, for instance, Fe or Ru has recently been addressed by Guo et al. [37]. The author [38] described the formation [39] of ammonia

consists of six elementary reactions which fell into the groups of activation, hydrogenation and desorption. The atomic centre-based classification of such electrocatalyst has its functionality. For instance, one metal centre is activating the nitrogen molecule, and the next center's task is to guide away activated nitrogen to form ammonia by a hydrogenation reaction.

Molten salt-based electrolysis has additional advantages concerning water-based electrolyte where hydrogen evolution reaction is a competing step with ammonia generation. However, direct synthesis of ammonia involves the production of hydrogen due to the difficulty in supplying proton and electrons to meet the chemical potential demand at the same time. Following this, the Jaramillo group at Stanford for the first time proposed a lithium recycling strategy to generate ammonia, and this process can be scaled up for centralized application. The process separates the nitrogen reduction step from the protonation step to generate the  $\text{NH}_3$  [40]. The process takes place in three steps. Electrolysis of molten  $\text{LiOH}$  produces lithium metal, which then reacts with nitrogen to complete the lithium nitridation step. Then ammonia is released from  $\text{Li}_3\text{N}$  in an exothermic hydrolysis reaction. Finally,  $\text{LiOH}$  is recycled back thus completing the cycle. With an applied bias of  $-4\text{V}$  at  $450^\circ\text{C}$ , they achieve up to 85% Faradaic efficiency for ammonia generation. The bias potential is the main parameter to control the evolution of hydrogen.

So far we have described the electrochemical ammonia synthesis at high temperature. Is it feasible to do this at ambient temperature? Most of the research in the current state of the art is related to carry out the NRR at low temperature. To achieve the same, Centi et al. [30] developed a  $\text{Fe}_2\text{O}_3/\text{CNT}$  electrocatalyst system for a gas-liquid-solid three-phase configuration. The membrane is designed in such a way that ammonia cannot cross from the cathode to the anode. In that study, the higher negative voltage is used to increase the Faradaic efficiency. Following this, iron supported by CNT was also used as electrocatalyst for ammonia generation at room temperature [30]. The rate of ammonia formation was  $2.2 \times 10^{-3} \text{ g m}^{-2} \text{ h}^{-1}$  with a DC bias of  $-2.0\text{V}$ . The electrocatalysts show stable behavior for 60 hrs of the reaction.

Recently electrochemical synthesis of ammonia is given attention in the conceptual design of solar ammonia refinery. Unlike in the Haber-Bosch process, where the necessary hydrogen is supplied by fossil fuels, "solar ammonia" uses PV to produce hydrogen by water electrolysis to the so-called green ammonia refinery process [41]. Noble metal-free electrocatalysts are also used in ambient conditions to fix nitrogen or generate ammonia besides Pt-based catalysts [39]. For example, a Bismuth based  $\text{Bi}_4\text{O}_{11}\text{V}_2/\text{CeO}_2$  electrocatalyst is designed as a cathode for NRR reaction. The role of  $\text{CeO}_2$  is to assist in the charge transfer process due to the proper band alignment with  $\text{Bi}_4\text{O}_{11}\text{V}_2$ . This system shows good Faradaic efficiency of 10.16%.

Boron-doped graphene nanosheets were used for the electrochemical ammonia synthesis in aqueous media. The material is supposed to have an electrocatalytic center, where Boron doping helps in the electron distribution in the graphene network. A doping level of 6.2% results in the 10.8 % Faradaic efficiency at 0.5 V [38]. 2D Boron nanosheets were used in neutral media, and it shows a Faradaic efficiency of 4.04% to enhance the selectivity for ammonia generation [42]. Density functional theory calculations suggest that oxidized and H-deactivated nanosheets are more effective than a pristine analogue of Boron nanosheet.

Before moving to more advanced system and the associated concept of electrochemical ammonia production, we make a note about the recent work of Andersen et al. [43], who established a robust and rigorous analytical methodology for the quantification of ammonia. It is a common artefact that in most of the case of ammonia generation, the amount produced is significantly small and it can be a source of contamination from air, human breath and ion-conducting polymeric membrane used in the electrochemical reactor or other labile nitrogen-containing compounds of  $\text{NO}$ ,  $\text{NO}_2^-$ ,  $\text{NO}_3^-$ , amine. The concept is based on the measurement of  $^{15}\text{N}_2$  isotope, and it helps in the reliable detection of  $\text{NH}_3$ . While this study mentions that the ammonia generation should not be from labile compounds such as nitrate, in recent studies it is evident that the electrochemical ammonia synthesis can

also be accomplished by eight electron-mediated reduction of nitrate into ammonia by using a copper-based molecular solid organometallic catalyst [44]. That author found that the copper incorporation into 3, 4, 9, 10- perylene tetracarboxylic acid dianhydride shows a Faradaic efficiency of 85.9% at -0.4 V. Another concept involves “ $\pi$ -back donation” and is mimicked to enhance the performance of ammonia production [45]. Here, authors have used P-block elemental catalysts lacking d-orbitals in compounds such as  $\text{Bi}_4\text{O}_5\text{I}_2$  as an electrocatalyst. This system helps in reducing the energy barrier associated with  $\text{N}_2$  protonation. Due to the advantage of the electronic modulation, this system shows a Faradaic efficiency of 32.4%. A comparative overview of the critical parameters of different electrocatalysts for accomplishing NRR reaction is summarized in table 1.

All the above example of NRR with available electrocatalysts leads to an efficiency scale not suitable for direct industrial application. Therefore, better engineering of electrocatalyst with good catalytic turnover and faradaic efficiency is the need of the hour to fulfill the demand of ammonia as a fuel, which is considered as generation 3 technology [42].

Table1: Comparison of different electrocatalysts performance

Catalyst	Temperature	Voltage	Efficiency	cost	Ref
molten hydroxide suspension of nano- $\text{Fe}_2\text{O}_3$	200°C	1.2V	35%	Not available	[29]
$\text{Fe}_2\text{O}_3/\text{AC}$ (activated carbon) catalysts	250°C	1.55V	13.7%	low-cost	[32]
Boron doped graphene	Room Temperature	-0.5V	10.8%	Not available	[34]
noble-metal-free $\text{Bi}_4\text{O}_{11}\text{V}_2/\text{CeO}_2$	Room Temperature	-0.2V	10.16%	Not available	[35]

hybrid					
Boron nanosheet	Room temperature	-0.8V	4.04%	Not available	[38]
copper-incorporated crystalline 3,4,9,10-perylenetetracarboxylic dianhydride.	Room Temperature	-0.4V	85.9%	Not available	[40]
Bi <sub>4</sub> O <sub>5</sub> I <sub>2</sub> (VO-Bi <sub>4</sub> O <sub>5</sub> I <sub>2</sub> -OH),	Room Temperature	-0.1 V	32.54%	Not available	[41]

### Development of soft X-ray spectroscopy for molecular structure analyses

The metal ions have been of eminent interest since 100 years because those are being used in technical inorganic catalysts in industrial chemistry. Therefore, much of the catalysis studies focussed on the electronic and molecular structure of typical 3d and 4d metals such as Fe, Ni, Cu, and Mo, V in their intimate bonding with ligand ions such as oxygen and nitrogen (also 5d row elements like Pt, Ru, Pd and the like). One of the easiest tasks to be performed with x-ray spectroscopy is the determination of the oxidation states of the metals. The x-ray absorption and emission spectroscopy of the 3d metal K-edges (K-shell absorption threshold) and later also their L-edges (L-shell absorption threshold) is meanwhile well developed [46] and available as research tool at synchrotron radiation centres [47]. Less well-known are the ligand spectra with O, N, S, P, and C, notwithstanding that the experiment and theory are well established [48]. There is a wealth of catalysts available for countless reactions in heterogeneous catalysis. However, little is known about their actual functionality at the molecular level.

In most of the studies, synchrotron-based X-ray spectroscopy techniques such as X-ray absorption spectroscopy (XAS) and X-ray emission absorption spectroscopy (XES) have been used to investigate the chemical signatures of elements in the process of nitrogen reduction reaction (NRR) [49-51].

The first Fe single site catalysts for NRR was reported by Lü et al. [52]. In this work bimetallic Fe/Zn zeolitic imidazolate frameworks were fabricated using hydrothermal methods. X-ray absorption near-edge structure (XANES) was used to probe the atomic structure of the Fe sites, and found that the Fe atom average valence is between  $\text{Fe}^{2+}$  and  $\text{Fe}^{3+}$ .

Guo and co-workers have used XAS and XES to probe the nitrogen bonding structure since more than two decades ago. The resonant X-ray emission spectra were studied early in 1996 by tuning the excitation energies to the five lowest vibrational levels of the  $\pi^*$  resonance [49]. This was the first time the resonant XES of  $\text{N}_2$  was presented. This was also an excellent illumination of several significant dipole selection rules because of the homonuclear diatomic nature of  $\text{N}_2$  and its closed-shell electronic structure. Additionally, the symmetry can be derived from the angle-resolved spectra. The influence of angular anisotropy and the parity selection rule on the intensity ratios of the absorption peaks in the fluorescence yield measurement of  $\text{N}_2$  can be predicted based on the information derived from resonant and non-resonant emission spectra. The nitrogen bonded with other elements are also investigated, e.g., the  $\text{CN}_x$  thin films prepared by magnetron sputtering [50]. Three different nitrogen bonding environments were investigated including nitriles (N1), pyridine-like N (N2) and nitrogen substituted graphite (N3). The N1 nitrogen has a sharp at 399.5 eV, originating from the  $\pi^*$  character. The N2 nitrogen is connected to two carbon atoms and has a feature peak at 398.5 eV. The N3 nitrogen with one  $\text{sp}^3$  carbon as a neighbor shows a peak at 401.7 eV, attributing to a low-energy  $\sigma^*$  resonance. The probing of nitrogen coordination in ionic liquids under in-situ/operando conditions were also achieved by Guo et al. using soft XAS [53]. As shown in Figure 7A, the N K-edge XAS has several signature peaks. The peak at 402 eV is sharp, attributing to the N1s to the  $\pi^*$  orbital of the imidazolium ring [54]. The transitions from  $\sigma^*$  orbitals of both cations and



anions is revealed in Figure 7B and 7C, as depicted by the other broader features in the peak deconvolution. The open and closed cell exhibit noticeable differences in their XAS spectra. The  $\pi^*$  resonance peak diminished over the 120 min while two peaks at 398.9 and 400.0 eV emerged. Combined with DFT calculations, the authors claimed the X-ray irradiation leads to the cleavage of C-N bonds, and corresponding removal of the alkyl groups adjacent to the imidazole ring. This study contributes to the understanding of the irradiation damage of the ionic liquids and reminds researchers to practice caution when investigating electrochemical or catalytic systems under *operando/in-situ* conditions using X-ray spectroscopies.

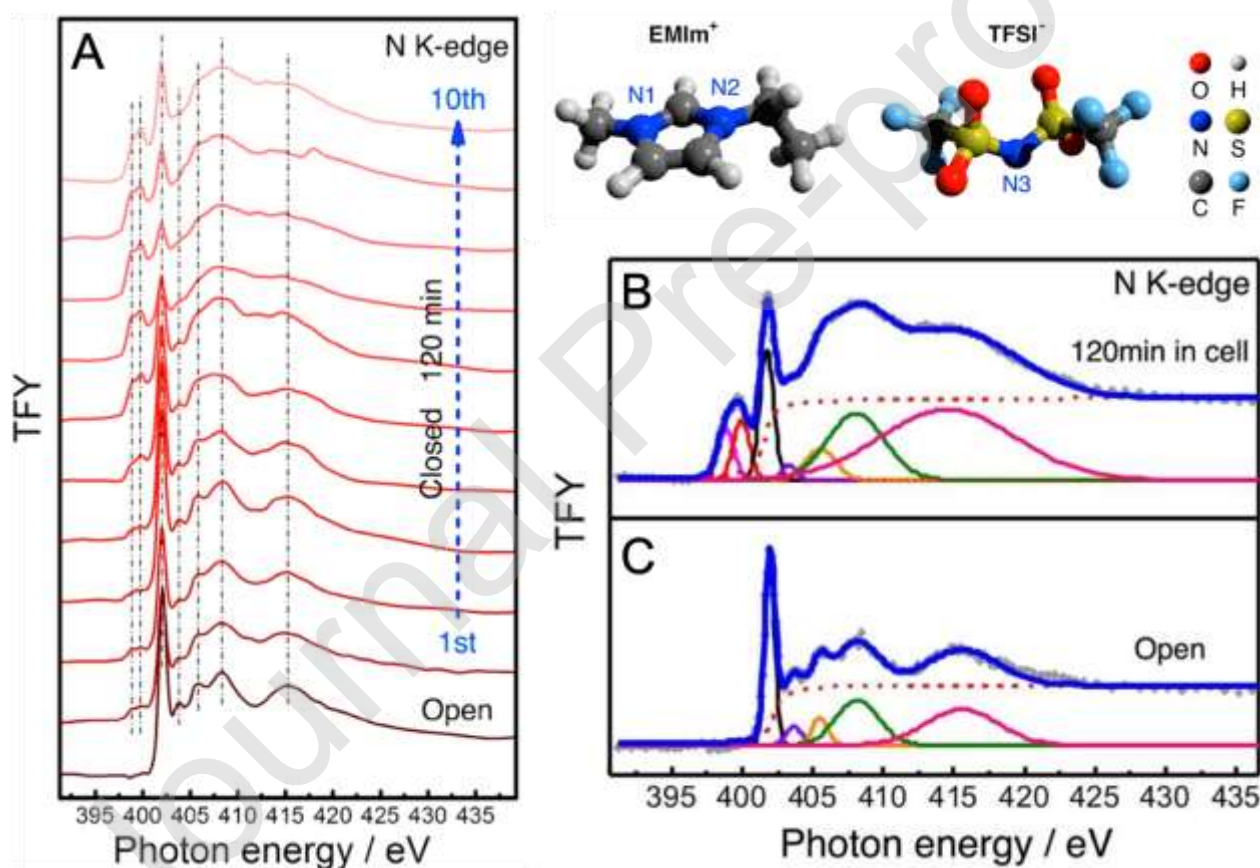


Figure 7. (A) Time-lapsed experimental N K-edge XAS spectra acquired from an encapsulated ionic liquid sample with that acquired with the open ionic liquid droplet in vacuum (bottom). Peak deconvolution of N K-edge spectra collected in (B) in the closed geometry after 120 min exposure and

(C) in the open geometry. Adapted from Ref. [53] with permission from the American Chemical Society.

In the electrochemical synthesis of ammonia, XAS was heavily employed as an effort to understand the local chemical and electronic environment. Examples of such electrochemical NRR catalysts include metals and alloys [55, 56], metal oxides [39, 57], metal chalcogenides [58-60], metal carbides [61], and recently reported metal phosphides [62]. Catalysts with active sites created by doping [63], single-atom dispersion [64, 65], oxygen [66] or nitrogen [67] vacancies are also reported. In most of these innovations, XAS plays an important role to probe and elucidate the chemical and electronic structures. For example, X-ray absorption near-edge structure (XANES) identified a new absorption peak of  $\text{-C}\equiv\text{N}$  for NPC-500 after the NRR compared to that before [68], indicating the creation of nitrogen vacancies which will become the active sites for NRR in the matrix [69]. Similarly, nitrogen vacancies in 2D nanosheet,  $\text{W}_2\text{N}_3$ , at the atomic level is probed by the extended X-ray absorption fine structure (EXAFS). Compared a  $\text{W}_2\text{N}_3$  nanosheet with and without vacancies, both samples show a main coordination peak near 2.8 Å assigned to W-W bonding [70], while the nitrogen vacant nanosheet XAS become weaker at 1.8 Å compared to that without vacancies, denoting a decreased W-N bonding number [67]. In a separate study of CoS/graphene, XANES spectra validate the construction of strong bridging bonds (Co-N/S-C) at the interface between  $\text{CoS}_x$  nanoparticles and nitrogen and sulfur-doped reduced graphene [71]. An element-specific technique with sensitivity to the local chemical and electronic environment, XAS can be applied to amorphous and crystalline samples, making it a powerful tool in the study of NRR catalysis.

Over time, scientists have become aware that the large protein complexes, which make up life, have a distinct shape (which can be destroyed by denaturation processes) and contain a vibration structure, a form, which is followed by a mechanical function, which is instrumental for driving the biochemical reactions. Such observation can invoke the concept of the responsive matrix [72], this

is, the multitude of functional components such as light antennas, light absorbers, charge separators, catalysts which respond to external stimuli and interact with the other components of the system for the conversion of water and carbon dioxide to hydrocarbons and biochemical intermediates and waste compounds, such as oxygen, and ammonia

With increasing complexity of the structure of such complexes, conventional vibration spectroscopy like Raman and infrared spectroscopy, fails to identify the role of key atoms in the molecules and their particular functions.

### **Nuclear resonant vibrational spectroscopy**

Nuclear resonant vibrational spectroscopy (NRVS) is a synchrotron radiation based nuclear scattering method that measures the creation (Stokes) or annihilation (anti-Stokes) of vibrations which are associated with the nuclear transition, *e.g.* at 14.414 keV for  $^{57}\text{Fe}$ . Figure 8(a) shows the principle of NRVS: while an incident X-ray beam scans through an interested energy region around the nuclear resonance, the nuclear back radiation (including the direct nuclear fluorescence  $h\nu_1$  and the converted electron fluorescence  $h\nu_2$ ) can be monitored as the NRVS signal [73]. The extremely monochromatic (*e.g.* 0.8 meV) incident energy can be tuned via a high-resolution monochromator (HRM) at a synchrotron nuclear scattering beamline, such as the ones shown in Figure 8(b) and (c), the scattering energy is precisely selected by the 5 neV ( $5 \times 10^{-9}$  eV) natural linewidth of the nuclear back radiation, while the NRVS signal (lifetime  $\approx$  nanoseconds) can be well separated from the electronic scattering (lifetime  $\approx$  femtoseconds) in the time domain, without the need for a low throughput diffraction spectrometer. NRVS spectra therefore have zero background and start from a true zero  $\text{cm}^{-1}$ . Even extremely weak NRVS feature, such as a 0.1 cts/s peak, is extractable from the huge electronic scattering background (in the order of 20 million cts/s).

In addition, NRVS has a number of compelling advantages over the established methods. For example: it is water transparent in comparison with far IR spectroscopy and thus well suitable for

studies of biological samples in their natural aqueous environment; it is free of fluorescence problems in comparison with resonance Raman spectroscopy and thus suitable for studies of photosensitive states; it well distinguishes among O, N and C in comparison with EXAFS. Most extraordinarily, NRVS is isotope (*e.g.*  $^{57}\text{Fe}$ ) specific and therefore it is almost a perfect tool to pin-point the site-specific information inside a complex molecule, such as nitrogenase [73].

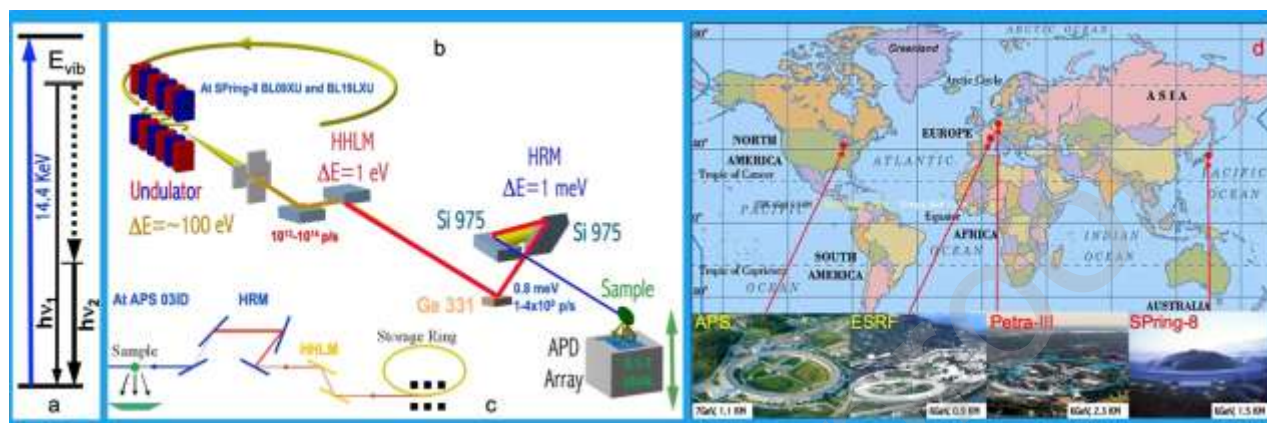


Figure 8: A nuclear excitation and de-excitation energy diagram (a); an experimental setup for NRVS measurements, from synchrotron radiation (SR) to NRVS measurement at SPring-8 (b) and APS (c); The SR centers which have nuclear scattering beamlines for NRVS experiments in Lemont Illinois, Hamburg, Grenoble, Hyogo (d).

The raw NRVS spectra are obtained as the counts from the delayed nuclear event (signal at  $h\nu_1$  and  $h\nu_2$ ) vs. the vibrational energy. It can be converted into partial vibrational density of state (PVDOS), which is a pure molecular property and can be further explored via normal mode analysis (NMA) or density functional theory (DFT) simulations to evaluate the proposed theoretical model(s) as well as the corresponding reaction mechanism(s). Even without theoretical simulations, the frequencies and vibrational peak profiles can be identified intuitively in many cases (based on the comparison with known NRVS spectra) [26, 73].

Unlike other X-ray spectroscopies, NRVS needs a nuclear resonant scattering beamline which is available currently only at APS at Argonne Lab (Lemont IL), SPring-8 in Hyogo, ESRF in Grenoble,

and Petra-III in Hamburg. Nevertheless, due to its super advantages, its user community as well as the research results shoots up fast. It becomes the third modern X-ray spectroscopy, which are widely accepted by the biochemical researchers, following x-ray crystallography and EXAFS.

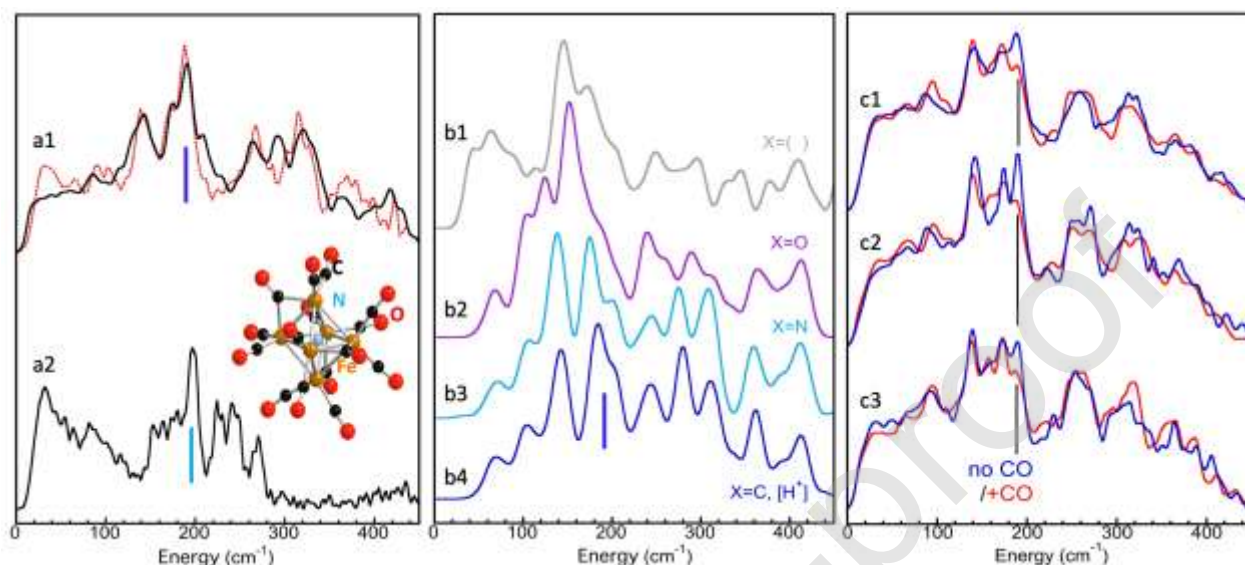


Figure 9: (a1) NRVs of isolated FeMo-co (black) vs. M-center obtained via (MoFe protein – P cluster) difference spectrum (dashed red); (a2) NRVs of the model complex ion  $[\text{Fe}_6\text{N}](\text{CO})_{15}]^{3-}$  while the right insert is the structure of this complex ion; (b) DFT calculated NRVs spectra assuming a central atoms of (b1) no atom, (b2) O, (b3) N, and (b4) C; (c) observed NRVs for a series of nitrogenase samples [(c1) wild type (WT); (c2)  $\alpha\text{-H195Q}$ ; (c3) photolysis on WT, with CO (red) vs. without CO (blue)].

Using molybdenum iron nitrogenase as example, the whole enzyme is divided into iron protein and molybdenum iron (MoFe) protein, which contains M-center and P-cluster. Although the nitrogen fixation involves all these components, many publications indicate M-center is the substrate binding site and therefore the critical site for nitrogen fixation. This M-center can also be extracted into NMF solvent as FeMo-co. It has a caged structure with a trunk of central  $\text{Fe}_6\text{X}$  core in the middle, one Mo on one end and one Fe at the other end, as shown in Figure 5 (bottom). The  $^{57}\text{Fe}$  specific NRVs is suitable to study this complicated structure. Here we illustrate two important examples: 1)



the investigation of the central atom X inside the caged FeMo-co structure; and 2) the binding structure of substrate CO to FeMo-co cage.

In 2007, several years before the structural identification of the central atom inside nitrogenase, NRVS was able to suggest a possible N or C atom for X [26]. As shown in Figure 9(a1), NRVS of extracted FeMo-co (black) or that of M-center obtained via (MoFe protein – P cluster) difference spectrum (dashed red) shows a characteristic peak at around  $190\text{ cm}^{-1}$  [indicated with a dark blue bar in Figure 9 (a1)], which does not overlap with any of Fe–S peaks when compared it with many Fe–S proteins and complexes. Further comparison with the model complex ion  $[\text{Fe}_6\text{N}](\text{CO})_{15}]^{3-}$  shows that the model has 1) a central core structure of  $\text{Fe}_6\text{N}$ , which is similar with the central core of FeMo-co ( $\text{Fe}_6\text{X}$ , where X is still not known at that time but was proposed as N by most scientists); 2) Its NRVS spectrum also has a characteristic peak around  $196\text{ cm}^{-1}$  indicated with a light blue bar (a2). Detailed evaluation shows that this peak is belong to the shaking mode of the  $\text{Fe}_6\text{X}$  or  $\text{Fe}_6\text{N}$  [26]. This observation is very important. With NRVS we thus can do "listening" to the FeMo-co-factor versus the FeS cluster in nitrogenase and deriving information on the partial vibration DOS which reflects the catalytic  $\text{N}\equiv\text{N} \rightarrow \text{NH}_3$  reaction. The insert in Figure 9(a2) is the structure of this complex ion  $[\text{Fe}_6\text{N}](\text{CO})_{15}]^{3-}$ .

As this characteristic peak is the  $\text{Fe}_6\text{X}$  shaking mode [26], its detailed spectral profile should be affected by what atom is inside the cage. Then DFT vs. NRVS can be an excellent tool to assist the identification of the central atoms. As shown in Figure 9(b), DFT calculation assuming no atom (b1), O(b2), N(b3), and C(d4) are performed. Among all, the DFT calculation assuming C(b4) or N(b3) provide excellent results in comparison of the observed NRVS for FeMo-co or M-center (a1). Therefore, NRVS can tell what atom is inside the FeMo-co cage.

Furthermore, binding substrate will distort the cage symmetry and therefore will affect the profile of this characteristic peak. Since  $\text{N}_2/\text{N}$  or  $\text{H}_2/\text{H}$  bound nitrogenase is hard to produce and extract in pure and large amount, CO is often used as alternative substrate in the research of nitrogenase–



substrate binding structures. Figure 9(c) is for a series of observed NRVS spectra for nitrogenase enzymes without substrate (blue) and those with CO substrate (red): (c1) is for the wild type (WT)  $Av_2$  nitrogenase; (c2) is for the  $\alpha$ -H195Q mutant  $Av_2$  nitrogenase (H195Q for short); (c3) is for the WT  $Av_2$  nitrogenase + CO and its photolysis product (CO dissociated). These spectra well-illustrated that nitrogenase molecules without substrate have a sharp and high peak at about 190–200  $\text{cm}^{-1}$  while the ones with CO bound have an obvious lower intensity in this characteristic peak [74]. This peak becomes an indirect but often useful indication that the nitrogenase has a substrate bound to.

In addition to this indirect observation, direct observation on Fe–CO structure with NRVS is also possible. Fe–CO features for WT  $Av_2$  nitrogenase+CO is illustrated as in Figure 10(b) while the ones for WT  $Av_2$  nitrogenase+ $^{13}\text{CO}$  is as in 10(a) [74]. There are about 9–10  $\text{cm}^{-1}$  red shift between them, experimentally identifying these peaks as Fe–CO. The pair of NRVS spectra for  $\alpha$ -H195Q  $Av_2$  nitrogenase+ $^{13}\text{CO}$  / +CO are illustrated in Figure 10(c) and (d). We can see the  $\alpha$ -H195Q pair has much more prominent Fe–CO features (including more resolved and more intense peaks) in comparison with the WT pair. This is because the  $\alpha$ -H195Q nitrogenase+ $^{12/13}\text{CO}$  has much high production yield in comparison with the WT nitrogenase+ $^{12/13}\text{CO}$ .

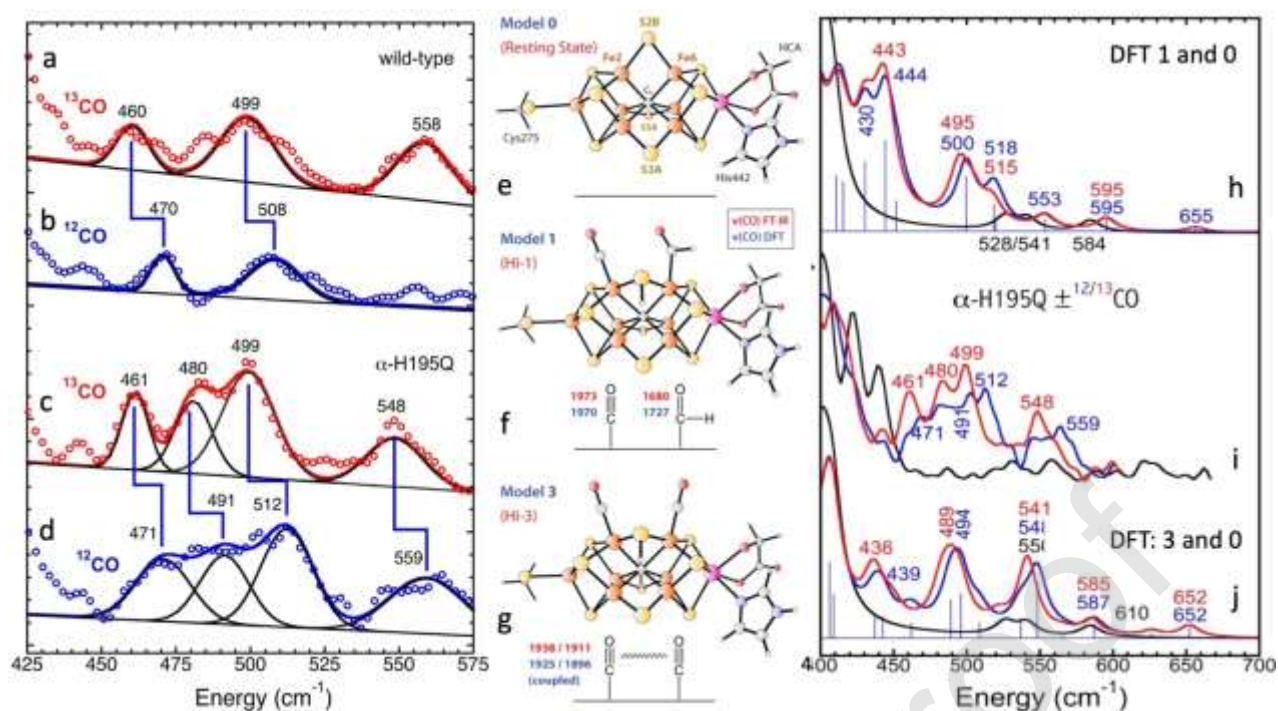


Figure 10: NRVs of  $^{13}\text{CO}$  (a) and CO (b) bound wild type (WT) nitrogenase vs.  $^{13}\text{CO}$  (c) and CO (d) bound  $\alpha$ -H195Q nitrogenase in the Fe-CO region (425–575  $\text{cm}^{-1}$ ); Structural models 0 (e), 1 (f) and 3 (g) used for DFT calculation on NRVs of as-isolated, WT+CO and  $\alpha$ -H195Q+CO nitrogenases respectively; DFT calculated (or observed) NRVs for as-isolated (black) vs. CO (blue) and  $^{13}\text{CO}$  (red) bound nitrogenases: (h) DFT calculation on WT and WT+CO using model 0 (black) and 1 (blue and red); (i) observed NRVs for  $\alpha$ -H195Q nitrogenase (black), + CO (blue) and +  $^{13}\text{CO}$  (red); and (j) DFT calculation on  $\alpha$ -H195Q and  $\alpha$ -H195Q+CO using model 0 (black) and 3 (blue and red).

The detailed Fe-CO spectra provide a good basis for DFT calculation and for Fe-CO structural evaluation from DFT calculations. Several Fe-CO binding models have been proposed in the middle panel, while DFT calculation using these models are shown as in the right panel [74]. Model 0 has no CO and it is used to calculate the as-isolated states (black curves) for WT (h) and  $\alpha$ -H195Q nitrogenases (i); Model 1 has one CO bound to Fe2 and one HCO bound to Fe6 positions, which is consistent with the FTIR frequencies of and the simulated NRVs for WT+CO here (h). Model 3 has

each CO at Fe2 and Fe6, which is consistent with the FTIR frequencies of the simulated NRVS for  $\alpha$ -H195Q+CO here (j). In comparison of (i) vs (j), it is clear that the observed NRVS spectra are well reproduced via DFT calculation. We thus understand that the NRVS difference between the WT+CO and  $\alpha$ -H195Q+CO is mainly due to their difference in Fe–CO binding structures. DFT calculation in combination with NRVS is also a critical tool to pinpoint the iron specific information in various other nitrogenases.

The 1.5 meV resolution inelastic X-ray scattering (IXS) on a series of Mo/V nitrogenase model complexes as well as on FeMo-cofactor were also examined at SPring-8 BL35XU. In addition to the  $^{57}\text{Fe}$  specific NRVS, IXS can provide information about the Mo site and the Mo related vibrational modes.

As the SR ring, beamtimes, detectors, experimental methods and sample preparation methods continue to progress, we believe, NRVS monitoring Fe–H/H<sub>2</sub> or Fe–N/N<sub>2</sub> structures or IXS monitoring on other metal (Mo) structures will become feasible in the future.

### **Nitrogen based ammonia fuel**

We want to close this review with an outlook on the potential expansion of the ammonia technology and business towards ammonia fuel. Given that around 80% of the world energy consumption is in the form of fuels, as opposed to electric energy [75], production of renewable fuels without net CO<sub>2</sub> emission will be essential for meeting the requirements of the Paris Accord signed in 2016. Elishav et al. argue that the economic potential of ammonia as fuel is vastly overlooked [76]. In the fossil-based economy and in synthetic hydrocarbon fuels, produced by renewable energy, carbon is the hydrogen carrier. Hydrogen as such has been identified as the essential component of a hydrogen economy [77, 78], but the storage and handling of H<sub>2</sub> gas has been considered a bottleneck for the necessary technology. Electric vehicles with fuel cells run on H<sub>2</sub> gas, compressed to up to 700 bar, and the fuel content is thus measured by mass, not volume [79]. 1 kg of H<sub>2</sub> contains 33.33 kWh

usable energy, and the fuel tank of fuel cell cars takes around 5 kg H<sub>2</sub>. The energy of NH<sub>3</sub> is only 5.22 kWh/kg, though, whereas 1 kg of gasoline has an energy content around 10 kWh. However, an aqueous solution of NH<sub>4</sub>OH and urea is a valuable liquid fuel, which can easily take it up with future large-scale energy storage technologies such as methanol and batteries. A consortium study from 2017 concludes that CO<sub>2</sub> neutral NH<sub>3</sub> produced with electrochemistry using sustainable electricity will be a feasible alternative for NH<sub>3</sub> produced from natural gas in the longer term [80].

Another aspect that deserves attention is the fact that biomass, when used for fuel production, is based at large on the use of ammonia fertilizer which until now are mainly produced by fossil fuels. So, there is a hidden portion of fossil fuel in biomass fuel, irrespective of its direct CO<sub>2</sub> neutrality. Huo et al. suggest [81] recycling ammonia to either plant or algal feedstock, so as to reduce the demand for synthetic fertilizer supplementation. This implies the closing of the nitrogen cycle. Zhang et al. [82] propose the use of a high temperature electrochemical ammonia synthesis route, with steam electrolysis being the route for H<sub>2</sub> production. The high temperature (thermal) "waste energy" can be utilised as the process heat to ammonia conversion (power-to-ammonia). They estimate the efficiency of this process to be 74%, as compared to biomass-to-ammonia with 44%, and methane-to-ammonia to 61%. When high temperature electrochemistry industry have a deeper market penetration, along with increased renewable electric power availability, the power-to-ammonia concept could be economically viable. Addressing, and solving the fuel problem, as the principal energy problem will likely remain the tallest order: energy supply shall be sustainable, available and affordable. But the management of the nitrogen atom in our civilization serves not only directly the food production and potentially the future fuel production, but also the synthesis of the various N-containing fine chemicals (in contrast to the bulk chemicals like urea, and ammonia) which are the building blocks of many other products important for our industrialized economy and society. Some of the N-containing molecules can be synthesized by "green" processes from biomass components. Examples are shown in the very recent review by He et al. [83].

## Competing financial interests

The authors declare no competing financial interests.

## Acknowledgement

This manuscript is a collaboration result of the EU H2020 SUNRISE Flagship Initiative [84], funded from the European Union's Horizon 2020 research and innovation programme under grant agreement No 816336. A. B. is grateful for the invitation to the Ertl Symposium on Surface Analysis and Dynamics 2014 to Berlin, by Jaeyoung Lee and Bongjin Simon Mun (GIST Korea), on the occasion of which the photo for the Haber-Bosch setup was taken. This research used resources of the ALS, a U.S. DOE Office of Science User Facility under contract no. DE-AC02-05CH11231. Some of the soft x-ray spectroscopy experiments were carried out on BL 6.3.1.2, 7.3.1, and 8.0.1 at Advanced Light Source (ALS). Research by L.L. and E.L. was funded by the Deutsche Forschungsgemeinschaft (DFG, German Research Foundation) under Germany's Excellence Strategy – EXC 2008 – 390540038 – UniSysCat., and the research project 405325648. SPC acknowledges support from NIH GM-65440. The NRVs and IXS experiments were performed at APS 03ID and SPring-8 BL09XU / BL35XU (via proposals 2013B0103, 2012B1577, and 2018A1033).

## References

- [1] E. Vitaku, D.T. Smith, J.T. Njardarson, Analysis of the structural diversity, substitution patterns, and frequency of nitrogen heterocycles among U.S. FDA approved pharmaceuticals, *Journal of Medical Chemistry*, 57 (2014) 10257-10274.
- [2] F. Wöhler, Ueber künstliche Bildung des Harnstoffs, *Annalen der Physik und Chemie*, 88 (1828) 253-256.

- [3] W. Prout, Observations on the Nature of some of the proximate Principles of the Urine; with a few remarks upon the means of preventing those diseases, connected with a morbid state of that fluid, *Medico-Chirurgical Transactions*, 8 (1817) 521-596 529.
- [4] M.R. Finlay, The Rehabilitation of an Agricultural Chemist: Justus Von Liebig and the Seventh Edition, *Ambix*, 38 (1991) 155-167.
- [5] N.K. Fageria, Green Manuring in Crop Production, *Journal of Plant Nutrition*, 30 (2007) 691-719.
- [6] J. Chang, J. Halliday, Mao. Das Leben eines Mannes. Das Schicksal eines Volkes., 4. Auflage ed., Karl Blessing Verlag, München, 2005.
- [7] I.A. Krupenikov, B.P. Boincean, D. Dent, The Past, Present and Future of the Chernozem, *The Black Earth: Ecological Principles for Sustainable Agriculture on Chernozem Soils*, Springer, Dordrecht NL, 2011, pp. 131-138.
- [8] S.W. Crookes, The wheat problem; based on remarks made in the presidential address to the British association at Bristol in 1898. Revised, with an answer to various critics, John Murray, Albemarle Street, London, 1899.
- [9] J.K. Nørskov, J. Chen, J. Goldstein, R. Miranda, T. Fitzsimmons, R. Stack, Sustainable Ammonia Synthesis - Exploring the scientific challenges associated with discovering alternative, sustainable processes for ammonia production, DOE Roundtable Report, Discussion held February 18, 2016, Dulles, VA, U.S. Department of Energy, Office of Science, 2016.
- [10] A. Braun, Quantum Electrodynamics of Photosynthesis - Mathematical Description of Light, Life and Matter, De Gruyter, Berlin, Boston, 2020.
- [11] Y. Lu, Y. Yang, T. Zhang, Z. Ge, H. Chang, P. Xiao, Y. Xie, L. Hua, Q. Li, H. Li, B. Ma, N. Guan, Y. Ma, Y. Chen, Photoprompted Hot Electrons from Bulk Cross-Linked Graphene Materials and Their Efficient Catalysis for Atmospheric Ammonia Synthesis, *ACS Nano*, 10 (2016) 10507-10515.
- [12] J.G. Chen, R.M. Crooks, L.C. Seefeldt, K.L. Bren, R.M. Bullock, M.Y. Darensbourg, P.L. Holland, B. Hoffman, M.J. Janik, A.K. Jones, M.G. Kanatzidis, P. King, K.M. Lancaster, S.V. Lyman, P. Pfromm, W.F. Schneider, R.R. Schrock, Beyond fossil fuel-driven nitrogen transformations, *Science*, 360 (2018).
- [13] Y. Tanabe, Y. Nishibayashi, Developing more sustainable processes for ammonia synthesis, *Coordination Chemistry Reviews*, 257 (2013) 2551-2564.
- [14] A.J. Martín, T. Shinagawa, J. Pérez-Ramírez, Electrocatalytic Reduction of Nitrogen: From Haber-Bosch to Ammonia Artificial Leaf, *Chemistry*, 5 (2019) 263-283.
- [15] F. Haber, R. Le Rossignol, Über die Technische Darstellung von Ammoniak aus den Elementen, *Zeitschrift für Elektrochemie*, 19 (1913) 53-72.
- [16] F. Haber, Nobel Lecture 1920: The synthesis of ammonia from its elements, Nobel lectures including presentation speeches and laureates' biographies *Chemistry*, 1901/21, Elsevier Publishing Company, Amsterdam - London - New York, 1966.



- [17] L. Casale, R. Leprestre, Apparatus for the catalytic synthesis of ammonia, in: U.S.P. Office 1'478'550, United States, 1922.
- [18] Casale, Advanced Ammonia Casale Technologies for Ammonia Plants, NPC Tehran 2002, CASALE SA, Tehran, 2002, pp. 1-35.
- [19] A. Hermann, Haber und Bosch: Brot aus Luft - Die Ammoniaksynthese, Physik Journal, 21 (1965) 168-171.
- [20] A.K. Choudhary, S.K. Thakur, V.K. Suri, Technology Transfer Model on Integrated Nutrient Management Technology for Sustainable Crop Production in High-Value Cash Crops and Vegetables in Northwestern Himalayas, Communications in Soil Science and Plant Analysis, 44 (2013) 1684-1699.
- [21] V. Smil, Detonator of the population explosion, Nature, 400 (1999) 415-415.
- [22] J. Kong, A. Lim, C. Yoon, J.H. Jang, H.C. Ham, J. Han, S. Nam, D. Kim, Y.E. Sung, J.H. Choi, Electrochemical Synthesis of  $\text{NH}_3$  at Low Temperature and Atmospheric Pressure Using a  $\gamma\text{-Fe}_2\text{O}_3$  Catalyst, ACS Sustainable Chemistry & Engineering, 5 (2017) 10986–10995.
- [23] M.A. Shipman, M.D. Symes, Recent progress towards the electrosynthesis of ammonia from sustainable resources, Catalysis Today, 286 (2017) 57-68.
- [24] A. Braun, Electrochemical Energy Systems - Foundations, Energy Storage and Conversion, Walter de Gruyter GmbH, Boston, Berlin, 2019.
- [25] D.P. Hickey, R. Cai, Z.Y. Yang, K. Grunau, O. Einsle, L.C. Seefeldt, S.D. Minter, Establishing a Thermodynamic Landscape for the Active Site of Mo-Dependent Nitrogenase, Journal of the American Chemical Society, 141 (2019) 17150-17157.
- [26] Y.M. Xiao, K. Fisher, M.C. Smith, W.E. Newton, D.A. Case, S.J. George, H.X. Wang, W. Sturhahn, E.E. Alp, J.Y. Zhao, Y. Yoda, S.P. Cramer, How nitrogenase shakes - Initial information about P-cluster and FeMo-cofactor normal modes from nuclear resonance vibrational Spectroscopy (NRVS), Journal of the American Chemical Society, 128 (2006) 7608-7612.
- [27] E. Endoh, J.K. Leland, A.J. Bard, Heterogeneous photoreduction of nitrogen to ammonia on tungsten oxide, The Journal of Physical Chemistry, 90 (1986) 6223-6226.
- [28] R.L. Cook, A.F. Sammells, Ambient temperature gas phase electrochemical nitrogen reduction to ammonia at ruthenium/solid polymer electrolyte interface, Catalysis Letters, 1 (1988) 345-349.
- [29] V. Kordali, G. Kyriacou, C. Lambrou, Electrochemical synthesis of ammonia at atmospheric pressure and low temperature in a solid polymer electrolyte cell, Chemistry Communications, (2000) 1673-1674.
- [30] S. Chen, S. Perathoner, C. Ampelli, C. Mebrahtu, D. Su, G. Centi, Room-Temperature Electrocatalytic Synthesis of  $\text{NH}_3$  from  $\text{H}_2\text{O}$  and  $\text{N}_2$  in a Gas–Liquid–Solid Three-Phase Reactor, ACS Sustainable Chemistry & Engineering, 5 (2017) 7393-7400.

- [31] T. Murakami, T. Nohira, T. Goto, Y.H. Ogata, Y. Ito, Electrolytic ammonia synthesis from water and nitrogen gas in molten salt under atmospheric pressure, *Electrochimica Acta*, 50 (2005) 5423-5426.
- [32] J.G. Howalt, T. Vegge, Electrochemical ammonia production on molybdenum nitride nanoclusters, *Physical Chemistry Chemical Physics*, 15 (2013) 20957-20965.
- [33] S. Licht, B. Cui, B. Wang, F.F. Li, J. Lau, S. Liu, Ammonia synthesis. Ammonia synthesis by N<sub>2</sub> and steam electrolysis in molten hydroxide suspensions of nanoscale Fe<sub>2</sub>O<sub>3</sub>, *Science*, 345 (2014) 637-640.
- [34] S. Giddey, S.P.S. Badwal, A. Kulkarni, Review of electrochemical ammonia production technologies and materials, *International Journal of Hydrogen Energy*, 38 (2013) 14576-14594.
- [35] V. Kyriakou, I. Garagounis, E. Vasileiou, A. Vourros, M. Stoukides, Progress in the Electrochemical Synthesis of Ammonia, *Catalysis Today*, 286 (2017) 2-13.
- [36] B. Cui, J. Zhang, S. Liu, X. Liu, W. Xiang, L. Liu, H. Xin, M.J. Lefler, S. Licht, Electrochemical synthesis of ammonia directly from N<sub>2</sub> and water over iron-based catalysts supported on activated carbon, *Green Chemistry*, 19 (2017) 298-304.
- [37] J. Guo, P. Chen, Catalyst: NH<sub>3</sub> as an Energy Carrier, *Chemistry*, 3 (2017) 709-712.
- [38] X. Yu, P. Han, Z. Wei, L. Huang, Z. Gu, S. Peng, J. Ma, G. Zheng, Boron-Doped Graphene for Electrocatalytic N<sub>2</sub> Reduction, *Joule*, 2 (2018) 1610-1622.
- [39] C. Lv, C. Yan, G. Chen, Y. Ding, J. Sun, Y. Zhou, G. Yu, An Amorphous Noble-Metal-Free Electrocatalyst that Enables Nitrogen Fixation under Ambient Conditions, *Angewandte Chemie International Edition*, 57 (2018) 6073-6076.
- [40] J.M. McEnaney, A.R. Singh, J.A. Schwalbe, J. Kibsgaard, J.C. Lin, M. Cargnello, T.F. Jaramillo, J.K. Nørskov, Ammonia synthesis from N<sub>2</sub> and H<sub>2</sub>O using a lithium cycling electrification strategy at atmospheric pressure, *Energy & Environmental Science*, 10 (2017) 1621-1630.
- [41] L. Wang, M. Xia, H. Wang, K. Huang, C. Qian, C.T. Maravelias, G.A. Ozin, Greening Ammonia toward the Solar Ammonia Refinery, *Joule*, 2 (2018) 1055-1074.
- [42] X. Zhang, T. Wu, H. Wang, R. Zhao, H. Chen, T. Wang, P. Wei, Y. Luo, Y. Zhang, X. Sun, Boron Nanosheet: An Elemental Two-Dimensional (2D) Material for Ambient Electrocatalytic N<sub>2</sub>-to-NH<sub>3</sub> Fixation in Neutral Media, *ACS Catalysis*, 9 (2019) 4609-4615.
- [43] S.Z. Andersen, V. Colic, S. Yang, J.A. Schwalbe, A.C. Nielander, J.M. McEnaney, K. Enemark-Rasmussen, J.G. Baker, A.R. Singh, B.A. Rohr, M.J. Statt, S.J. Blair, S. Mezzavilla, J. Kibsgaard, P.C.K. Vesborg, M. Cargnello, S.F. Bent, T.F. Jaramillo, I.E.L. Stephens, J.K. Nørskov, I. Chorkendorff, A rigorous electrochemical ammonia synthesis protocol with quantitative isotope measurements, *Nature*, 570 (2019) 504-508.
- [44] G.-F. Chen, Y. Yuan, H. Jiang, S.-Y. Ren, L.-X. Ding, L. Ma, T. Wu, J. Lu, H. Wang, Electrochemical reduction of nitrate to ammonia via direct eight-electron transfer using a copper–molecular solid catalyst, *Nature Energy*, 5 (2020) 605-613.

- [45] C. Lv, L. Zhong, Y. Yao, D. Liu, Y. Kong, X. Jin, Z. Fang, W. Xu, C. Yan, K.N. Dinh, M. Shao, L. Song, G. Chen, S. Li, Q. Yan, G. Yu, Boosting Electrocatalytic Ammonia Production through Mimicking " $\pi$  Back-Donation", *Chemistry*, 6 (2020) 2690-2702.
- [46] F. de Groot, A. Kotani, *Core Level Spectroscopy of Solids*, CRC Press 2008.
- [47] A. Braun, *X-ray Studies on Electrochemical Systems - Synchrotron Methods for Energy Materials*, Walter De Gruyter GmbH, Berlin/Boston, 2017.
- [48] J. Stöhr, *NEXAFS Spectroscopy*, Springer-Verlag, Berlin Heidelberg, 1992.
- [49] P. Glans, P. Skytt, K. Gunnelin, J.H. Guo, J. Nordgren, Selectively excited X-ray emission spectra of N<sub>2</sub>, *Journal of Electron Spectroscopy and Related Phenomena*, 82 (1996) 193-201.
- [50] N. Hellgren, J. Guo, C. S  the, A. Agui, J. Nordgren, Y. Luo, H.   gren, J.-E. Sundgren, Nitrogen bonding structure in carbon nitride thin films studied by soft x-ray spectroscopy, *Applied Physics Letters*, 79 (2001) 4348-4350.
- [51] R.S. Weatherup, B. Eren, Y. Hao, H. Bluhm, M.B. Salmeron, Graphene Membranes for Atmospheric Pressure Photoelectron Spectroscopy, *Journal of Physical Chemistry Letters*, 7 (2016) 1622-1627.
- [52] F. L  , S. Zhao, R. Guo, J. He, X. Peng, H. Bao, J. Fu, L. Han, G. Qi, J. Luo, X. Tang, X. Liu, Nitrogen-coordinated single Fe sites for efficient electrocatalytic N<sub>2</sub> fixation in neutral media, *Nano Energy*, 61 (2019) 420-427.
- [53] H. Wang, C.H. Wu, R.S. Weatherup, B. Feng, Y. Ye, Y.S. Liu, P.A. Glans, J. Guo, H.T. Fang, M.B. Salmeron, X-ray-Induced Fragmentation of Imidazolium-Based Ionic Liquids Studied by Soft X-ray Absorption Spectroscopy, *Journal of Physical Chemistry Letters*, 9 (2018) 785-790.
- [54] F. Rodrigues, D. Galante, G.M. do Nascimento, P.S. Santos, Interionic interactions in imidazolic ionic liquids probed by soft X-ray absorption spectroscopy, *Journal of Physical Chemistry B*, 116 (2012) 1491-1498.
- [55] Y.-C. Hao, Y. Guo, L.-W. Chen, M. Shu, X.-Y. Wang, T.-A. Bu, W.-Y. Gao, N. Zhang, X. Su, X. Feng, J.-W. Zhou, B. Wang, C.-W. Hu, A.-X. Yin, R. Si, Y.-W. Zhang, C.-H. Yan, Promoting nitrogen electroreduction to ammonia with bismuth nanocrystals and potassium cations in water, *Nature Catalysis*, 2 (2019) 448-456.
- [56] Z. Geng, Y. Liu, X. Kong, P. Li, K. Li, Z. Liu, J. Du, M. Shu, R. Si, J. Zeng, Achieving a Record-High Yield Rate of 120.9  $\mu\text{gNH}_3 \text{ mgcat.}^{-1} \text{ h}^{-1}$  for N<sub>2</sub> Electrochemical Reduction over Ru Single-Atom Catalysts, *Advanced Materials*, 30 (2018) e1803498.
- [57] M.M. Shi, D. Bao, B.R. Wulan, Y.H. Li, Y.F. Zhang, J.M. Yan, Q. Jiang, Au Sub-Nanoclusters on TiO<sub>2</sub> toward Highly Efficient and Selective Electrocatalyst for N<sub>2</sub> Conversion to NH<sub>3</sub> at Ambient Conditions, *Advanced Materials*, 29 (2017) 1606550-1606555.
- [58] X. Li, T. Li, Y. Ma, Q. Wei, W. Qiu, H. Guo, X. Shi, P. Zhang, A.M. Asiri, L. Chen, B. Tang, X. Sun, Boosted Electrocatalytic N<sub>2</sub> Reduction to NH<sub>3</sub> by Defect-Rich MoS<sub>2</sub> Nanoflower, *Advanced Energy Materials*, 8 (2018) 1-8.

- [59] B.H.R. Suryanto, D. Wang, L.M. Azofra, M. Harb, L. Cavallo, R. Jalili, D.R.G. Mitchell, M. Chatti, D.R. MacFarlane, MoS<sub>2</sub> Polymorphic Engineering Enhances Selectivity in the Electrochemical Reduction of Nitrogen to Ammonia, *ACS Energy Letters*, 4 (2018) 430-435.
- [60] J. Li, S. Chen, F.J. Quan, G.M. Zhan, F.L. Jia, Z.H. Ai, L.Z. Zhang, Accelerated Dinitrogen Electroreduction to Ammonia via Interfacial Polarization Triggered by Single-Atom Protrusions, *Chemistry*, 6 (2020) 885-901.
- [61] H. Cheng, L.X. Ding, G.F. Chen, L. Zhang, J. Xue, H. Wang, Molybdenum Carbide Nanodots Enable Efficient Electrocatalytic Nitrogen Fixation under Ambient Conditions, *Advanced Materials*, 30 (2018) e1803694.
- [62] S.L. Chen, H. Jang, J. Wang, Q. Qin, X. Liu, J. Cho, Bimetallic metal-organic framework-derived MoFe-PC microspheres for electrocatalytic ammonia synthesis under ambient conditions, *Journal of Materials Chemistry A*, 8 (2020) 2099-2104.
- [63] C.J. Zhao, S.B. Zhang, M.M. Han, X. Zhang, Y.Y. Liu, W.Y. Li, C. Chen, G.Z. Wang, H.M. Zhang, H.J. Zhao, Ambient Electrosynthesis of Ammonia on a Biomass-Derived Nitrogen-Doped Porous Carbon Electrocatalyst: Contribution of Pyridinic Nitrogen, *ACS Energy Letters*, 4 (2019) 377-383.
- [64] B. Yu, H. Li, J. White, S. Donne, J. Yi, S. Xi, Y. Fu, G. Henkelman, H. Yu, Z. Chen, T. Ma, Tuning the Catalytic Preference of Ruthenium Catalysts for Nitrogen Reduction by Atomic Dispersion, *Advanced Functional Materials*, 30 (2019) 1905665-1905675.
- [65] R. Zhang, L. Jiao, W.J. Yang, G. Wan, H.L. Jiang, Single-atom catalysts templated by metal-organic frameworks for electrochemical nitrogen reduction, *Journal of Materials Chemistry A*, 7 (2019) 26371-26377.
- [66] F.L. Lai, J.R. Feng, X.B. Ye, W. Zong, G.J. He, C. Yang, W. Wang, Y.E. Miao, B.C. Pan, W.S. Yan, T.X. Liu, I.P. Parkin, Oxygen vacancy engineering in spinel-structured nanosheet wrapped hollow polyhedra for electrochemical nitrogen fixation under ambient conditions, *Journal of Materials Chemistry A*, 8 (2020) 1652-1659.
- [67] H. Jin, L. Li, X. Liu, C. Tang, W. Xu, S. Chen, L. Song, Y. Zheng, S.Z. Qiao, Nitrogen Vacancies on 2D Layered W<sub>2</sub>N<sub>3</sub>: A Stable and Efficient Active Site for Nitrogen Reduction Reaction, *Advanced Materials*, 31 (2019) e1902709.
- [68] K.G. Latham, W.M. Dose, J.A. Allen, S.W. Donne, Nitrogen doped heat treated and activated hydrothermal carbon: NEXAFS examination of the carbon surface at different temperatures, *Carbon*, 128 (2018) 179-190.
- [69] S. Mukherjee, D.A. Cullen, S. Karakalos, K. Liu, H. Zhang, S. Zhao, H. Xu, K.L. More, G. Wang, G. Wu, Metal-organic framework-derived nitrogen-doped highly disordered carbon for electrochemical ammonia synthesis using N<sub>2</sub> and H<sub>2</sub>O in alkaline electrolytes, *Nano Energy*, 48 (2018) 217-226.
- [70] H. Yu, X. Yang, X. Xiao, M. Chen, Q. Zhang, L. Huang, J. Wu, T. Li, S. Chen, L. Song, L. Gu, B.Y. Xia, G. Feng, J. Li, J. Zhou, Atmospheric-Pressure Synthesis of 2D Nitrogen-Rich Tungsten Nitride, *Advanced Materials*, 30 (2018) e1805655.

- [71] P. Chen, N. Zhang, S. Wang, T. Zhou, Y. Tong, C. Ao, W. Yan, L. Zhang, W. Chu, C. Wu, Y. Xie, Interfacial engineering of cobalt sulfide/graphene hybrids for highly efficient ammonia electrosynthesis, *Proceedings of the National Academy of Sciences of the United States of America*, 116 (2019) 6635-6640.
- [72] R.L. Purchase, H.J. de Groot, Biosolar cells: global artificial photosynthesis needs responsive matrices with quantum coherent kinetic control for high yield, *Interface Focus*, 5 (2015) 20150014-20150029.
- [73] H. Wang, E. Alp, Y. Yoda, S.P. Cramer, A Practical Guide for Nuclear Resonance Vibrational Spectroscopy (NRVS) of Biochemical Samples and Model Compounds, in: J.C. Fontecilla-Camps (Ed.) *Methods in molecular biology*, Clifton, N.J. 2014, pp. 125-137.
- [74] A.D. Scott, V. Pelmeshnikov, Y.S. Guo, L.F. Yan, H.X. Wang, S.J. George, C.H. Dapper, W.E. Newton, Y. Yoda, Y. Tanaka, S.P. Cramer, Structural Characterization of CO-Inhibited Mo-Nitrogenase by Combined Application of Nuclear Resonance Vibrational Spectroscopy, Extended X-ray Absorption Fine Structure, and Density Functional Theory: New Insights into the Effects of CO Binding and the Role of the Interstitial Atom, *Journal of the American Chemical Society*, 136 (2014) 15942-15954.
- [75] A. Thapper, S. Styring, G. Saracco, A.W. Rutherford, B. Robert, A. Magnuson, W. Lubitz, A. Llobet, P. Kurz, A. Holzwarth, S. Fiechter, H. de Groot, S. Campagna, A. Braun, H. Bercegol, V. Artero, Artificial Photosynthesis for Solar Fuels - an Evolving Research Field within AMPEA, a Joint Programme of the European Energy Research Alliance, *Green*, 3 (2013) 43-57.
- [76] O. Elishav, D.R. Lewin, G.E. Shter, G.S. Grader, The nitrogen economy: Economic feasibility analysis of nitrogen-based fuels as energy carriers, *Applied Energy*, 185 (2017) 183-188.
- [77] D.P. Gregory, A Hydrogen-Energy System, American Chemical Society Symposium on NonFossil Chemical Fuels 9-14 April 1972, Institute of Gas Technology and American Gas Association, Washington D.C., 1972, pp. 446.
- [78] D.P. Gregory, D.Y.C. Ng, G.M. Long, The Hydrogen Economy, in: J.O. Bockris (Ed.) *Electrochemistry of Cleaner Environments*, Springer, Boston MA, 1972, pp. 226-280.
- [79] A. Braun, Von der Nordsee bis Venedig: Mit Wasserstoff und Brennstoffzelle Europa "erfahren". Eine "Auto"-Biographie., Erste Auflage ed., Kindle Direct Publishing, Zürich, 2019.
- [80] J. Witte, Power to Ammonia - Feasibility study for the value chains and business cases to produce CO<sub>2</sub>-free ammonia suitable for various market applications, Institute for Sustainable Process Technology, Amersfoort, The Netherlands, 2017.
- [81] Y.X. Huo, D.G. Wernick, J.C. Liao, Toward nitrogen neutral biofuel production, *Current Opinion in Biotechnology*, 23 (2012) 406-413.
- [82] H. Zhang, L. Wang, J. Van herle, F. Maréchal, U. Desideri, Techno-economic comparison of green ammonia production processes, *Applied Energy*, 259 (2020) 114135-114146.

[83] J. He, L. Chen, S. Liu, K. Song, S. Yang, A. Riisager, Sustainable access to renewable N-containing chemicals from reductive amination of biomass-derived platform compounds, *Green Chemistry*, 22 (2020) 6714-6747.

[84] A. Abbott, Europe's next euro1-billion science projects: six teams make it to final round, *Nature*, 566 (2019) 164-165.

Journal Pre-proof